Topological Magnetic Isomers

DOI: 10.1002/anie.201203309

Crystal-to-Crystal Transformation of Magnets Based on Heptacyanomolybdate(III) Involving Dramatic Changes in Coordination Mode and Ordering Temperature**

*Qing-Lun Wang, Heather Southerland, Jian-Rong Li, Andrey V. Prosvirin, Hanhua Zhao, and Kim R. Dunbar**

Crystal-to-crystal transformation is an interesting phenomenon with potential applications in molecular devices such as switches and sensors.[1] The structural changes typically involve minor movements of atoms in the crystal prompted by changes in metal coordination number, condensation reactions, rearrangement of bonds, or the removal or exchange of solvents.[1] It is challenging, however, to obtain high-quality crystals after solid-state transformations, especially those involving the breaking and formation of chemical bonds.[2–5] Some rare examples are single-crystal transformations of coordination polymers that change their dimensionality, such as 1D to 2D, 1D to 3D, and 2D to 3D.[3] as well as 0D compounds to 1D and 2D coordination polymers.[4]

Although various crystal-to-crystal transformations have been reported in recent years, very few examples involve drastic changes in the magnetic properties.[4a,5] In the course of our research into the properties of the heptacyanomolybdate(III) anion we isolated the 3D material $\{[Mn(dpop)]_3[Mn(dpop)(H_2O)][Mo(CN)_7]_2\cdot 13.5\,H_2O\}_n$ (**1**; dpop = 2,13-dimethyl-3,6,9,12,18-pentaazabicyclo[12.3.1]-octadeca-1(18),2,12,14,16-pentaene), which undergoes a remarkable single-crystal to single-crystal transformation to afford $\{[Mn(dpop)]_2[Mo(CN)_7]\cdot 2\,H_2O\}_n$ (**2**) by partial loss of solvent molecules with concomitant rearrangement of the binding mode of the heptacyanomolybdate linker. The alterations in the structure results in dramatic changes in the coercive field and ordering temperature of the magnet.

Compound **1** was prepared by slow diffusion of solutions of $K_4[Mo^{III}(CN)_7]$ and $[Mn^{II}(dpop)]Cl_2$ in the dark under a nitrogen atmosphere; the related phase, **2**, was prepared by subjecting crystals of **1** to a dynamic vacuum at 125 °C for 8 h and further pumping using the "outgas" function of a gas adsorption analyzer for 5 h at 150 °C.

[*] Dr. Q.-L. Wang, H. Southerland, Dr. J.-R. Li, Dr. A. V. Prosvirin, Dr. H. Zhao, Prof. Dr. K. R. Dunbar
Department of Chemistry, Texas A&M University
College Station, TX 77842 (USA)
E-mail: dunbar@mail.chem.tamu.edu
Homepage: http://www.chem.tamu.edu/rgroup/dunbar/
Dr. Q.-L. Wang
Department of Chemistry, Nankai University
Tianjin, 300071 (P.R. China)

[**] This work was supported by the U.S. Department of Energy (DE-FG02-02ER45999) and the National Natural Science Foundation of China (no. 21071085).

Supporting information for this article is available on the WWW under http://dx.doi.org/10.1002/anie.201203309.

Crystals of **1** belong to the rhombohedral space group $R\bar{3}$. The crystallographically independent unit consists of a $\{[Mn^{III}(dpop)]_3[Mn^{II}(dpop)(H_2O)][Mo(CN)_7]_2\}$ fragment (Figure 1a) and interstitial water molecules. It can be seen from

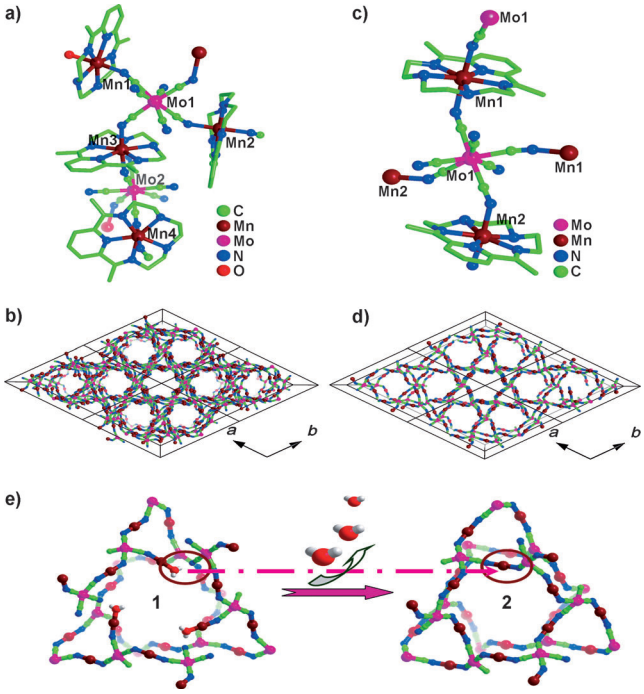

Figure 1. a) The basic structural unit $\{[Mn(dpop)]_3[Mn(dpop)(H_2O)][Mo(CN)_7]_2\}$ in **1** (H atoms are omitted for clarity). b) The 3D architecture of **1** viewed along the *c* direction. c) The basic structural unit $\{[Mn(dpop)]_2[Mo(CN)_7]\}$ in **2** (H atoms are omitted for clarity). d) The 3D architecture of **2** viewed along the *c* direction. e) Crystal-to-crystal transformation from **1** to **2**.

the asymmetric unit that both the Mo^{III} and Mn^{II} ions are heptacoordinate with slightly distorted pentagonal bipyramidal geometries. There are two types of Mn^{II} ions in the structure: the Mn1 center is surrounded by five nitrogen atoms of the macrocyclic dpop ligand in the equatorial positions as well as one bridging CN^- ion from the $[Mo(CN)_7]^{4-}$ ion and one H_2O molecule in the axial positions. This unit acts as a terminal capping group. In contrast, the Mn2, Mn3, and Mn4 centers are all bridged by two CN^- groups in the axial positions and function as μ-CN bridging units. The Mn–N bond distances range from 2.21 to 2.35 Å, which are very close to the literature values for other

$[Mn(dpop)]^{2+}$ species.[6] Among the $[Mo(CN)_7]^{4-}$ units, Mo1 is connected to four $[Mn(dpop)]^{2+}$ moieties, with two bridging CN^- ligands located in equatorial positions (N1, N4) and the other two in the axial sites (N2, N6). The Mo2 centers are connected to three $[Mn(dpop)]^{2+}$ units, with two bridging CN^- groups in the equatorial positions (N8, N12) and one in an axial postion (N10). The Mo–C bond lengths range from 2.07 to 2.19 Å and the Mo–C≡N bond angles are close to 180° (174–178°).

From a topological point of view, both Mo1 and Mo2 can be regarded as 3-connecting nodes and the $[Mn(dpop)]^{2+}$ moiety as a bridge, with a $[Mn(dpop)(H_2O)]^{2+}$ unit acting as a terminal fragment. The result is a non-uniform net with the vertex symbol $6,10^2$ and a Schläfli symbol $6.10^2.10^2$ (depicted schematically in Figure S1 in the Supporting Information; the topological analysis was performed with the TOPOS program package).[7] Thus, complex **1** has a highly ordered 3D framework architecture with 1D tubular channels of approximately 15 Å diameter (Figure 1b). The channels are directed along the *c* axis and are filled with H_2O guest molecules.

The crystallographically independent unit of compound **2** is composed of a $\{[Mn(dpop)]_2[Mo(CN)_7]_2\}$ fragment and two water molecules. As shown in Figure 1c, there is only one type of Mn^{II} ion in the asymmetric unit; although they are crystallographically independent, the Mn1 and Mn2 centers from the $[Mn(dpop)]^{2+}$ units both act as μ-CN bridging units and, in contrast to compound **1**, there is no terminal $[Mn(dpop)(H_2O)]^{2+}$ group. The Mo1 center is connected to four $[Mn(dpop)]^{2+}$ entities, with two bridging CN^- ligands located in equatorial positions (N3 and N7) and two in the axial positions (N1, N5). From a topological point of view, Mo1 is a 4-connecting node, with the $[Mn(dpop)]^{2+}$ moiety acting as a bridge, thereby resulting in a non-uniform topological net with the vertex symbol $6^4,8^2$ and Schläfli symbol $6^2.6^2.6^2.6^2.8^2.8^2$ (shown schematically in Figure S1 in the Supporting Information).[7] The result is a highly ordered 3D framework structure with 1D tubular channels of approximately 10 Å diameter (Figure 1d). The channels are directed along the *c* axis and are filled with H_2O guest molecules which are hydrogen bonded to the nitrogen atom of the $[Mo(CN)_7]^{4-}$ unit (O1···N4A 2.945 Å; O2···N2B 2.887 Å).

The major difference between **1** and **2** in regard to the network structure is that **1** contains a water-capped {Mn(dpop)} unit (Mn1) which is dehydrated and bridged by a cyanide group from the adjacent $[Mo(CN)_7]^{4-}$ moiety (Mo2; Figure 1e). As a result, the number of pathways of exchange interactions increases, which dramatically alters the magnetic properties (see below).

Magnetic data for the two new compounds were collected over the temperature range 2–300 K. Plots of χ_M^{-1} and $\chi_M T$ versus T for **1** are shown in Figure 2, where χ_M is the molar magnetic susceptibility per $Mo_2^{III}Mn_4^{II}$ unit. The value of $\chi_M T$ at 300 K is 18.15 $cm^3 K mol^{-1}$, which is very close to the spin-only value of 18.25 $cm^3 K mol^{-1}$ for four uncoupled high-spin Mn^{II} ($S = 5/2$) ions and two Mo^{III} ($S = 1/2$) ions if one assumes $g = 2.0$. When the temperature is lowered, the $\chi_M T$ value decreases smoothly from room temperature to 95 K and reaches a minimum value of 17.8 $cm^3 K mol^{-1}$. Below 95 K, the $\chi_M T$ value rapidly increases to reach a maximum value of

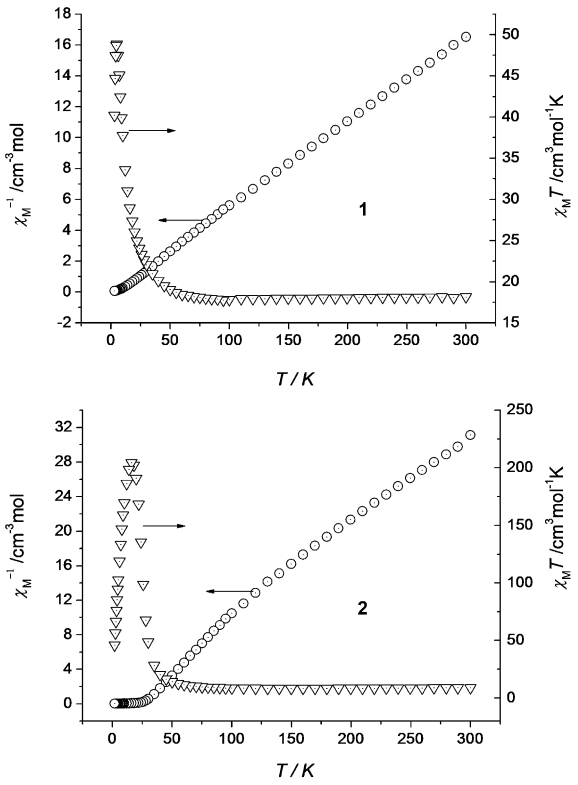

Figure 2. Plots of χ_M^{-1} (○) and $\chi_M T$ (▽) versus *T* of **1** (top) and **2** (bottom) from 2 to 300 K in an applied dc field of 1000 Oe.

48.9 $cm^3 K mol^{-1}$ at 5.0 K, then decreases rapidly to a value of 40.2 $cm^3 K mol^{-1}$ at 2 K. A fitting of the data above 95 K to the Curie–Weiss law gives $\theta = -2.5$ K, but, because of the complicated structure of complex **1**, it is not possible to evaluate the coupling constant between the Mn^{II} and Mo^{III} ions. The negative θ value and the decrease in the $\chi_M T$ value below 95 K both suggest that an antiferromagnetic coupling is operative between the Mn^{II} and Mo^{III} spin centers, a conclusion that is consistent with results of neutron diffraction studies on $Mn^{2+}[Mo(CN)_7]^{4-}$ compounds.[8] The antiferromagnetic interaction is also reflected by the magnetization data, which saturate at 2.0 K (see Figure S2 in the Supporting Information) to a value of 18.20 μ_B at 70 kOe. This value is in good agreement with the expected value of $S = 18/2$ per $Mo_2^{III}Mn_4^{II}$ unit (18.00 μ_B).

Figure 3 depicts a plot of the zero-field-cooled magnetization and field-cooled magnetization data at a field of 10 Oe. This plot shows a bifurcation of the data below 2.6 K, thus indicating the occurrence of long-range ordering below this temperature.[9] The field-cooled magnetization exhibits a plateau below this temperature, which is typical of a complete freezing process. Isothermal magnetization experiments performed at 1.8 K exhibit a hysteresis with a small coercive field of 90 Oe and a remnant magnetization of 0.26 $N\mu_B$, typical of soft magnet behavior.

Long-range ordering was also confirmed by ac susceptibility data measured at different frequencies in the range 1–1339 Hz in a zero applied dc field (see Figure S3 in the Supporting Information). The in-phase χ_M' and out-of-phase components χ_M'' both display maxima, clearly indicating the

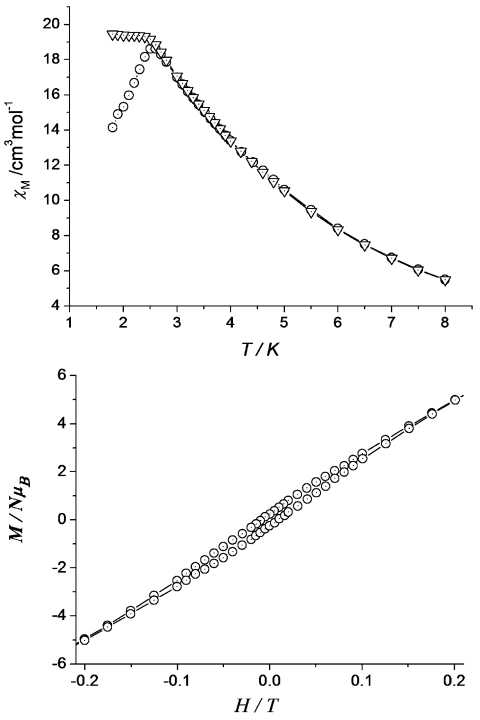

Figure 3. Top: Zero-field-cooled (ZFC; ○) magnetization and field-cooled (FC; ▽) magnetization curves for **1** in a dc field of 10 Oe. Bottom: Hysteresis loop of **1** at 1.8 K.

occurrence of 3D ferromagnetic ordering. A very small frequency dependence of the AC data was observed, with shifts in χ_M' from 2.8 to 3.3 K at frequencies ranging from 1 Hz to 1339 Hz. The shift parameter $\gamma = (\Delta T_p/T_p)/\Delta(\log f)$ (f = ac frequency) is approximately 0.052, which is close to a typical value for a spin-glass behavior. A more appropriate term for magnetically concentrated molecule-based magnets is a glassy magnet, which is a metastable state of frozen spins that does not undergo a true three-dimensional ordering. Nevertheless, these materials undergo a spontaneous magnetization and exhibit coercivity which classify them as magnets. Similar behavior has been observed in other magnetically ordered systems.[10]

Compound **2** exhibits a $\chi_M T$ value at 300 K of 9.02 $cm^3 K mol^{-1}$, which is slightly lower than the spin-only value of 9.13 $cm^3 K mol^{-1}$ for two uncoupled high-spin Mn^{II} ($S = 5/2$) ions and one Mo^{III} ($S = 1/2$) ion (χ_M here is the molar magnetic susceptibility per $Mo^{III}Mn^{II}_2$ unit). When the temperature is lowered, the $\chi_M T$ value decreases slightly from room temperature to 130 K and reaches a minimum value of 8.48 $cm^3 K mol^{-1}$. Below 130 K, the $\chi_M T$ value first increases steadily to 25 K and then increases abruptly to reach 204.3 $cm^3 K mol^{-1}$ at 16 K before finally decreasing rapidly to a value of 46.1 $cm^3 K mol^{-1}$ at 2 K. A fitting of the data above 130 K to the Curie–Weiss law gives $\theta = -16.0$ K, which is an indication of strong antiferromagnetic coupling between the Mn^{II} and Mo^{III} ions. The antiferromagnetic coupling was further confirmed by the magnetization data at 2 K (see Figure S2 in the Supporting Information), which show a steady increase to a near saturation value of 8.35 μ_B at 70 kOe, close to the expected value of $S = 9/2$ per $Mo^{III}Mn^{II}_2$ unit (9.0 μ_B).

As shown in Figure 4, the zero-field-cooled magnetization and field-cooled magnetization data at a 10 Oe indicate long-range ordering occurs for **2** with a critical temperature (T_C) of

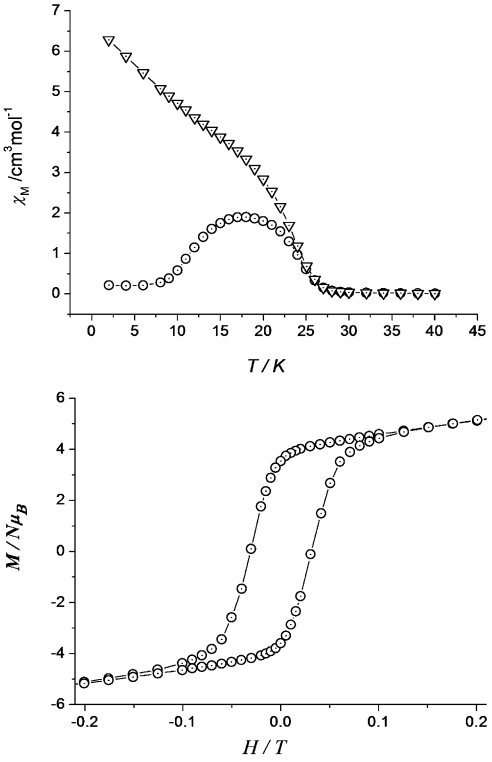

Figure 4. Top: Zero-field-cooled (ZFC; ○) magnetization and field-cooled (FC; ▽) magnetization curves for **2** under a dc field of 10 Oe. Bottom: Hysteresis loop of **2** at 1.8 K.

24 K.[9] Magnetization data at 1.8 K exhibit hysteresis with a much larger coercive field of 305 Oe than that observed for **1**, as well as a remnant magnetization of 3.6 $N\mu_B$, typical of a harder magnet. The magnetic ordering was confirmed by the ac data measured at different frequencies in a zero applied dc field. The in-phase and out-of-phase components exhibit maxima typical of 3D ordering (see Figure S4 in the Supporting Information), albeit with a small frequency dependence of the peaks T_p in the χ_M' and χ_M'' data (the shifts in χ_M' from 20 to 22 K are from 1 Hz to 1339 Hz and the parameter $\gamma = (\Delta T_p/T_p)/\Delta(\log f)$ is approximately 0.30), which means that complex **2** is similar to **1** in terms of glassy magnet behavior.

In summary, two nearly identical compositions of 3D crystalline materials based on $[Mo(CN)_7]^{4-}$ and $[Mn(dpop)]^{2+}$ have been prepared, with one phase, compound **2**, being generated from crystals of **1** by a dehydration process that involves a surprising crystal-to-crystal transformation with major rearrangements of the connectivity of the two building blocks in the structure. Magnetic measurements indicate that **1** is a typical soft magnet, whereas **2** displays a large coercive field and remnant magnetization. To our knowledge, such a drastic change in architecture and magnetic properties

triggered only by loss of water molecules and without compromising the integrity of the single crystals is without precedent. Such a discovery provides a rare opportunity for probing subtle structural factors that affect magnetic properties in related solids and is specifically important for testing models of binding modes and anisotropy in compounds based on the pentagonal bipyramidal heptacyanomolybdate(III) anion, a topic of high interest in magnetism research on cyanide compounds.

Experimental Section

All experiments were performed under a nitrogen atmosphere. Dark red needlelike crystals of **1** were obtained after a week by diffusion of solutions of $[Mn(dpop)]Cl_2 \cdot 4H_2O$[6a] (125 mg in 3 mL CH_3OH on the top), a CH_3OH/H_2O (1:1) mixture (16 mL, as a buffer in the middle), and $K_4[Mo(CN)_7] \cdot 2H_2O$[11] (60 mg in 3 mL H_2O at the bottom). Compound **2** was prepared by pumping on single-crystal samples of **1** under a dynamic vacuum at 125 °C for 8 h followed by further pumping for 5 h at 150 °C using the "outgas" function of a gas adsorption analyzer.

Thermogravimetric analysis was used to estimate the number of crystallized water molecules in **1** (see Figure S5 in the Supporting Information; 10.72 % weight loss, which is ca. 13.5 H_2O molecules per $Mo_2^{III}Mn_4^{II}$ unit).

Crystal data for **1**: $C_{74}H_{94.33}Mn_4Mo_2N_{34}O_{13.11}$, rhombohedral, space group $R\bar{3}$, $a = 32.089(3)$, $b = 32.089(3)$, $c = 53.420(11)$ Å, $\alpha = 90$, $\beta = 90$, $\gamma = 120°$. $V = 47\,637(12)$ Å^3, $Z = 18$, $T = 110$ K, $R_1 = 0.0832$ for 1183 parameters and 14 960 unique reflections with ($I > 2\sigma(I)$) and $R_1 = 0.1190$ for all 128 166 reflections with GOF = 1.024.

Crystal data for **2**: $C_{37}H_{46}Mn_2MoN_{17}O_2$, rhombohedral, space group $R3$, $a = 29.772(4)$, $b = 29.772(4)$, $c = 12.763(3)$ Å, $\alpha = 90$, $\beta = 90$, $\gamma = 120°$. $V = 9797(3)$ Å^3, $Z = 9$, $T = 110$ K, $R_1 = 0.0476$ for 536 parameters and 8007 unique reflections with ($I > 2\sigma(I)$) and $R_1 = 0.0702$ for all 31 531 reflections with GOF = 1.119.

CCDC 840101 for **1** and 866544 for **2** contain the supplementary crystallographic data for this paper. These data can be obtained free of charge from The Cambridge Crystallographic Data Centre via www.ccdc.cam.ac.uk/data_request/cif.

Received: April 30, 2012
Published online: August 15, 2012

Keywords: crystal-to-crystal transformation · heptacyanide · magnetic properties · molecular magnetism · molybdenum

[1] a) S. Kitagawa, R. Kitaura, S. Noro, *Angew. Chem.* **2004**, *116*, 2388 – 2430; *Angew. Chem. Int. Ed.* **2004**, *43*, 2334 – 2375; b) J. J. Vittal, *Coord. Chem. Rev.* **2007**, *251*, 1781 – 1795; c) J.-P. Zhang, X.-C. Huang, X.-M. Chen, *Chem. Soc. Rev.* **2009**, *38*, 2385 – 2396.

[2] a) A. Aslani, A. Morsali, M. Zeller, *Dalton Trans.* **2008**, 5173 – 5177; b) H. Sadeghzadeh, A. Morsali, *Inorg. Chem.* **2009**, *48*, 10871 – 10873; c) Z.-L. Fang, R.-M. Yu, X.-Y. Wu, J.-S. Huang, C.-Z. Lu, *Cryst. Growth Des.* **2011**, *11*, 2546 – 2552; d) W. M. Bloch, C. J. Sumby, *Chem. Commun.* **2012**, *48*, 2534 – 2536.

[3] a) C. H. Hu, U. Englert, *Angew. Chem.* **2005**, *117*, 2321 – 2323; *Angew. Chem. Int. Ed.* **2005**, *44*, 2281 – 2283; b) J. D. Ranford, J. J. Vittal, D. Wu, X. Yang, *Angew. Chem.* **1999**, *111*, 3707 – 3710; *Angew. Chem. Int. Ed.* **1999**, *38*, 3498 – 3501; c) E. Y. Lee, M. P. Suh, *Angew. Chem.* **2004**, *116*, 2858 – 2861; *Angew. Chem. Int. Ed.* **2004**, *43*, 2798 – 2801; d) S. K. Ghosh, W. Kanebo, D. Kiriya, M. Ohba, S. Kitagawa, *Angew. Chem.* **2008**, *120*, 8975 – 8979; *Angew. Chem. Int. Ed.* **2008**, *47*, 8843 – 8847; e) Z. Duan, Y. Zhang, B. Zhang, D. Zhu, *J. Am. Chem. Soc.* **2009**, *131*, 6934 – 6935.

[4] a) X.-N. Cheng, W.-X. Zhang, X.-M. Chen, *J. Am. Chem. Soc.* **2007**, *129*, 15738 – 15739; b) Y.-J. Zhang, T. Liu, S. Kanegawa, O. Sato, *J. Am. Chem. Soc.* **2009**, *131*, 7942 – 7943; c) Y.-J. Zhang, T. Liu, S. Kanegawa, O. Sato, *J. Am. Chem. Soc.* **2010**, *132*, 912 – 913; d) B. Zhang, D. Zhu, Y. Zhang, *Chem. Eur. J.* **2010**, *16*, 9994 – 9997.

[5] a) M. Kurmoo, H. Kumagai, K. W. Chapman, C. J. Kepert, *Chem. Commun.* **2005**, 3012 – 3014; b) D. Armentano, G. D. Munno, T. F. Mastropietro, M. Julve, F. Lloret, *J. Am. Chem. Soc.* **2005**, *127*, 10778 – 10779; c) X.-N. Cheng, W.-X. Zhang, Y.-Y. Lin, Y.-Z. Zheng, X.-M. Chen, *Adv. Mater.* **2007**, *19*, 1494 – 1498; d) S. M. Neville, G. J. Halder, K. W. Chapman, M. B. Duriska, P. D. Southon, J. D. Cashion, J.-F. Létard, B. Moubaraki, K. S. Murray, C. J. Kepert, *J. Am. Chem. Soc.* **2008**, *130*, 2869 – 2876; e) B. Zhang, D. Zhu, Y. Zhang, *Chem. Asian J.* **2011**, *6*, 1367 – 1371.

[6] a) O. Jiménez-Sandoval, D. Ramírez-Rosales, M. J. Rosales-Hoz, M. E. Sosa-Torres, R. Zamorano-Ulloa, *J. Chem. Soc. Dalton Trans.* **1998**, 1551 – 1556; b) G. Rombaut, S. Golhen, L. Ouahab, C. Mathonière, O. Kahn, *J. Chem. Soc. Dalton Trans.* **2000**, 3609 – 3614; c) C. Paraschiv, M. Andruh, Y. Journaux, Z. Žak, N. Kyritsakas, L. Ricard, *J. Mater. Chem.* **2006**, *16*, 2660 – 2668; d) D. Zhang, H. Wang, Y. Chen, Z.-H. Ni, L. Tian, J. Jiang, *Inorg. Chem.* **2009**, *48*, 5488 – 5496.

[7] V. A. Blatov, A. P. Shevchenko, V. N. Serezhkin, *J. Appl. Crystallogr.* **2000**, *33*, 1193; TOPOS software is available for download at http://www.topos.ssu.samara.ru.

[8] J. A. Stride, B. Gillon, A. Goukassov, J. Larionova, R. Clérac, O. Kahn, *C. R. Acad. Sci. Ser. IIc* **2001**, 105 – 112.

[9] a) C. M. Wynn, M. A. Gîrţu, J. Zhang, J. S. Miller, A. J. Epstein, *Phys. Rev. B* **1998**, *58*, 8508 – 8514; b) H.-L. Sun, Z.-M. Wang, S. Gao, *Chem. Eur. J.* **2009**, *15*, 1757 – 1764.

[10] a) C. V. Krishnamohan Sharma, C. C. Chusuei, R. Clérac, T. Möller, K. R. Dunbar, A. Clearfield, *Inorg. Chem.* **2003**, *42*, 8300 – 8308; b) R. Clérac, S. O'Kane, J. Cowen, X. Ouyang, R. Heintz, H. Zhao, M. J. Bazile, Jr., K. R. Dunbar, *Chem. Mater.* **2003**, *15*, 1840 – 1850; c) X. Liu, O. Roubeau, R. Clérac, *C. R. Chim.* **2008**, *11*, 1182 – 1191.

[11] R. C. Young, *J. Am. Chem. Soc.* **1932**, *54*, 1402 – 1405.

